31st Annual International Conference of the IEEE EMBS
Minneapolis, Minnesota, USA, September 2-6, 2009

A Univariate Model of Calcium Release in the Dyadic Cleft of Cardiac Myocytes

Junjie Fan and Zeyun Yu*, *Member, IEEE*

Abstract— **Local calcium sparks in the dyadic cleft of cardiac myocytes are triggered by calcium influxes via L-type calcium channels (LCCs) located on the transverse tubule (TT) membrane, and subsequently controlled by the regeneration of ryanodine receptors (RyRs) on the sarcoplasmic reticulum (SR). Calcium released from SR channels is known to be responsible for the sparks. Therefore, the activities of RyRs provide straightforward indication to the calcium concentration alteration. A method to study calcium signaling by analyzing RyR-gating statistics is described in the present study. Here we propose a univariate model with a simplified geometry of the dyadic cleft, which specifies the spatial localization of LCCs and RyRs to monitor the activity changes of RyRs. This model is used to explore two crucial aspects of local calcium signaling: the first is to disclose the tight control of calcium influxes via LCCs, and the second is to reveal the interactional impact of the self-regenerative RyRs. Patterns of active RyRs are rendered through numerous computational simulation experiments, manipulating the state initialization and the spatial localization of LCCs and RyRs to observe gating transition of RyRs.**

I. INTRODUCTION

LOCAL calcium concentration increase in intracellular calcium, known as "calcium sparks" [1], [13], is the elementary event for the global signaling, which is responsible for the skeletal and cardiac muscles' extension and contraction. In the dyadic space of cardiac cells, calcium influxes through L-type Calcium Channels (LCCs) trigger the neighboring ryanodine receptors (RyRs) to open, thereby releasing more calcium that subsequently stimulates other RyRs to open. Due to the decisive roles that LCCs and RyRs play in calcium signaling, the underlying control mechanisms are therefore of our great interests.

Over the past two decades, the local calcium signaling in muscles, neurons and cardiac cells has been researched from the aspects of both biology laboratory experiments and computer simulations. A number of studies on spark formation and detection, diffusion, amplitude and rise time variations with altered external biological conditions such as temperature [2], myosin light chain kinase and peptides [3] and β−adrenergic [4], or internal physical parameters such as the gap distance between the transverse tubule (TT) and sarcoplasmic reticulum (SR) membranes [5] and the density of LCCs and RyRs on membranes, have been conducted, while many issues at intracellular levels such as calcium signaling dynamics in the dyadic space still remain controversial. Our focus in this paper is to achieve an adequately comprehensive interpretation of local calcium dynamics. A computational simulation model is employed to explore the local control mechanisms of LCCs and RyRs. This model adopts the concept of fully stochastic discrete random walk in the dyadic cleft, which has been claimed to agree well with the deterministic continuous model [14]. Computer simulations in our work are performed with MCell, a Monte Carlo based tool for realistic modeling of cellular signaling in the complex three-dimensional (3D) sub-cellular microenvironment (www.mcell.cnl.salk.edu).

Cardiac contraction is contingent on the SR membrane excitation, called "excitation-contraction (EC) coupling" [2]. The event begins with cytoplasm calcium influxes via opened LCCs on the TT membrane which is depolarized by an electrical potential propagated throughout the cell membrane [6], [12]. Influent calcium subsequently diffuses through the dyadic cleft and activates calcium release from the closely apposed RyRs on the SR membrane. This regenerative process, known as calcium-induced calcium release (CICR) [7], amplifies the calcium signaling, which essentially leads to the sparks. To be more specific, two types of calcium, calcium influx via LCCs and calcium released from a cluster of RyRs, induce RyRs to release much more calcium. The overwhelming majority of calcium in the dyadic cleft is rapidly released from RyRs, which is the key event in the spark formation. Therefore, it is inferred that the activities of RyRs can indicate the calcium concentration alteration. A method is thus developed in the present paper to study the calcium signaling by analyzing the statistics of RyR state transition. One calcium release unit (CaRU) is simulated in the computational environment to study the phenomenon of calcium propagation by a simplified model based on the diffusion and control principles. This univariate model is proposed to study the effects of radial distances from an opened LCC to RyRs and radial distances from an opened RyR to the other neighboring RyRs, respectively.

The rest of this paper is organized as follows. Section II gives the methodological details of the geometric model of the dyadic cleft, the gating change diagram with parameters, indication of RyRs activities and a univariate model we developed to study calcium signaling in an individual calcium release unit (CaRU). We will present and discuss some results in Section III. Section IV concludes this paper and points out some limitation and future work of the current studies.

Manuscript received April 7, 2009. This work is supported in part by a subcontract from the National Biomedical Computation Resource (NIH P41 RR08605). J. Fan is supported in part by the AOP fellowship at University of Wisconsin-Milwaukee.

J. Fan and Z. Yu are with the Department of Computer Science, University of Wisconsin-Milwaukee, Milwaukee, WI 53211, USA.

*Corresponding author: Z. Yu (phone: 414-229-2960; fax: 414-229-6958; email: yuz@uwm.edu).

II. METHODS

A. The geometric model of the dyadic cleft

In skeletal and cardiac muscles, an interaction between junctional sarcoplasmic reticulum (jSR) and T-Tubular membranes occurs at individual calcium release units (CaRUs) [8]. The geometry of CaRUs is composed of T-Tubule and apposed junctional domains of sarcoplasmic reticulum (jSR). Two proteins that are critical to EC coupling are contained: (i) dihydropyridine receptors (DHPRs) or L-type calcium influx channels (LCCs), which reside on the T-Tubule membranes, and (ii) ryanodine receptors (RyRs) or calcium release channels, which are physically apposed on SR membranes ([8], [11]). LCCs are distributed in clusters on sarcolemmal membranes with no order in their arrangement, while RyRs are highly ordered on the apposed jSR [9]. Latest studies have shown that RyRs are approximately uniformly distributed. Although LCCs and RyRs are not structurally linked and there is a junctional gap between them, they are functionally associated in a single CaRU. Each LCC controls a cluster of RyRs by calcium permeation through the dyadic cleft space. Moreover, calcium from each CaRU disperses so rapidly that it usually does not trigger adjacent CaRUs to release calcium. Based on the above findings, we simulate an individual calcium release unit (CaRU) as an independent simple model which has two parallel surfaces to dispose LCCs and RyRs respectively. Here we have adopted the simple rectangular box model proposed by Koh et al. [5]. The cardiac dyadic cleft space has been estimated to span 0.05-0.2μm in radius and 12nm in height ([5], [9]). Recent cryo-EM imaging studies have shown that RyRs are approximately uniformly arranged and each RyR is a four-side symmetric molecule with a dimension around 27nm (the structure is shown in Figure 1 B). Therefore, in our model, the separation gap distance between the top and bottom surfaces, which stand for the TT and SR membranes respectively, is set to be 12nm.

The bottom surface (SR membrane) is composed of a number of equally-spaced small squares with a dimension of 27nm×27nm. In each small square, one RyR is placed, as shown in Figure 1A. LCCs are randomly distributed at the top surface (TT membrane) for the studies suggesting that LCCs be disordered.

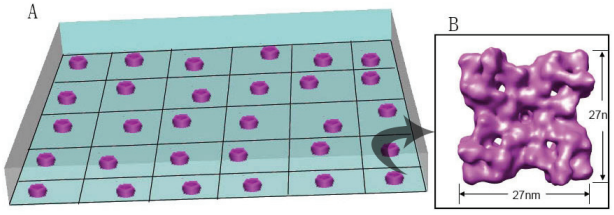

Figure 1 The geometry of the model and RyRs distribution. (A) The dyadic cleft is modeled as a rectangular space between TT membrane (Top Surface) and SR membrane (Bottom surface). The height of the space is 12nm. The bottom surface is composed of many small squares with a dimension of 27nm×27nm, each of which is assigned with one RyR. The number of squares (or RyRs) used varies in our models (see the main texts). (B) A 3D enlarged view of an individual RyR structure. The cryo-electron microscopy map was provided by Wah Chiu, BCM.

B. LCCs and RyRs gating diagrams and parameters

Stochastic gating of LCCs and RyRs changes with certain probabilities of reaction transition in terms of rate constants and it determines which transition will take place in the next time step. With the help of the state transition diagram and the probabilities, we are able to stimulate the stochastic process in the computer environment and to analyze it with Monte Carlo method. Here we adopt the schematic diagram integrated by Koh et al. [5].

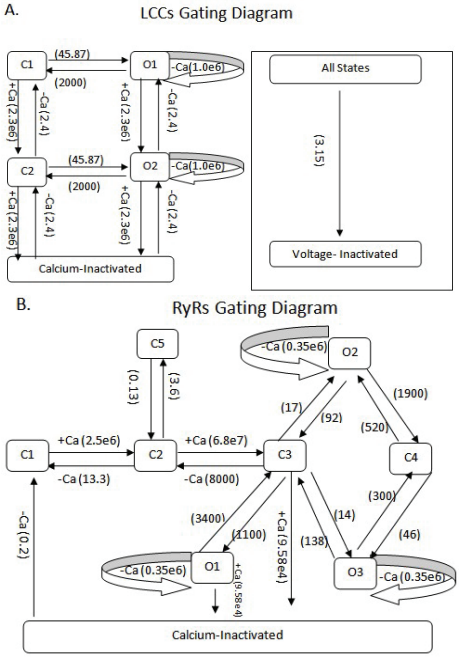

Figure 2 Schematic state diagrams adopted from the models described by Koh et al. [5]. State changes by either releasing calcium (denoted as "-Ca") or consuming calcium (denoted as "+Ca") in the binding/unbinding events. Each state changes at a time step with a certain probability, which is indicated in the bracket.

(A) Gating diagram and rate constant parameters for LCCs.

(B) Gating diagram and rate constant parameters for RyRs.

From the transition probabilities, we can tell that the majority of calcium release occurs at an open state to itself. The formation of a calcium spark is the result of the CICR, that is, released calcium from RyRs forms the spark. Therefore, the gating transition of RyRs is the key event in local calcium sparks.

C. RyRs activities indicating calcium signaling

Spontaneous calcium release attributes to the summed action of discretely distributed RyRs. From the above analysis, we propose that RyRs activities can be used as an indicator of calcium signaling. Among all the activated RyRs, the hyperactive RyRs provide the most contribution to the release of calcium ions, although some of the transitions between closed states do release a small amount of calcium too. In our model, we have considered the summation of all RyRs activities.

MCell keeps detailed records of gating status of every individual LCC and RyR at each time step. With this data, we are able to track the position and gating status of each LCC and RyR on different spatial and temporal scales, which are used to distinguish what specific changes have

taken place at a particular time and analyze how these changes influence calcium signaling in the local environment.

D. Univariate model

In the "cluster bomb" model proposed by Michal D. Stern, a cluster of SR channels (RyRs) are coupled to one "trigger" LCC and such a cluster is locally regenerative. Because the channels in a cluster are capable of sensing the calcium released from the opened channels nearby, they can be triggered to open in turn [6]. For the purpose to study this local control mechanism, we have developed a univariate model within a single CaRU to observe the triggering process of LCCs and the interactional stimulating control of opened RyRs.

To understand these two local control mechanisms, we are interested in: (i) studying the activities of RyRs with different radial distances to the opened LCC that is the source of the triggering calcium; (ii) observing how one hyperactive RyR (opened RyR) influences other RyRs within various radial distances. Our focus in this model is the role of the radial distance from an opened LCC to adjacent RyRs in the triggering process, and also the role of the radial distance from an opened RyR to other RyRs in the CICR process along with time variations.

In order to study how a variable affects the whole process, it is necessary to keep all the other conditions the same. To study the first aspect, we associate one initially opened LCC and a cluster of initially closed RyRs. For the second case, we place no LCC but one initially opened RyR at the center of a cluster of initially closed RyRs.

1) LCC triggering: To study this process, one initially opened LCC (LCC-O1 in Figure 2A) is placed at the center of the top surface and 100 initially closed RyRs (RyR-C1 in Figure 2B) at the bottom (10 RyRs on each row and 10 RyRs on each column), as shown in Figure 3.

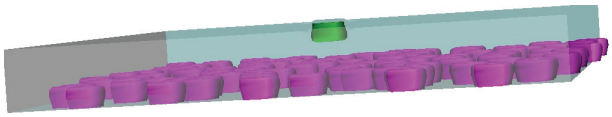

Figure 3 Layout and elements of the model to study LCC triggering mechanism. The height is 12nm, the dimension of the bottom and top is 270nm×270nm. A RyR is placed in each 27nm×27nm square. One opened LCC (the green particle) is placed at the center of top surface and 100 initially closed RyRs (the red particles) are distributed on the bottom.

Every RyR has a distance to the LCC (the green particle in Figure 3), and all these distances form a radial shape with the LCC as the source, similar to an "umbrella" structure. The behaviors of RyRs with different distances are recorded during the simulation.

2) RyR self-controlling regeneration: In order to have a better observation of RyR self-controlling regeneration, we start the simulation by assuming that one RyR has already been triggered to the open state (RyR-O1 in Figure 2B). Therefore, no LCC is considered in this experiment but instead, an initially opened RyR (RyR-O1 in Figure 2B and the green particle in Figure 4) is assumed at the center of a cluster of 440 initially closed RyRs (RyR-C1 in Figure 2B and the red particles in Figure 4). All the distances from the cluster of RyRs (red) to the initially opened RyR (green) form a concentric star-like shape.

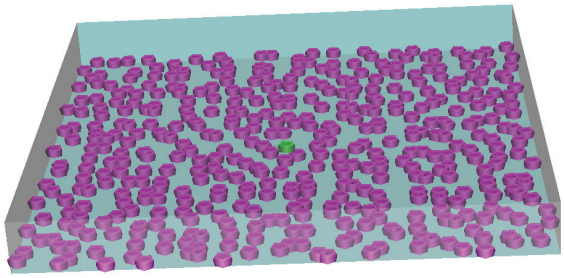

Figure 4 Layout and elements of the model to study the RyR self-controlling mechanism. The height is 12nm, the dimension of the bottom and top is 567nm×567nm (21 RyRs in each row and column; each RyR is located in a 27nm×27nm square). No LCC is considered. Alternatively one opened RyR (the green particle) is placed at the center of the bottom and 440 initially closed RyRs (the red particles) are distributed on the bottom. For a better view of this model, this image has been enlarged by 10 times in the height dimension.

III. RESULTS AND DISCUSSION

Calcium regulation and individual RyR and LCC activities are highly stochastic. In order to discover patterns and correlations between the LCC control and RyR self-response, the Monte Carlo method is used to simulate the associated behaviors. A large amount of data produced by numerous simulations is then mined and analyzed with customized C-programs. Different simulations with various time durations have been conducted and compared in order to discover the influence fluctuation of LCC triggering mechanism and RyR self-regeneration control. For each case with certain duration, 100 independent trials are carried out. In the model, the number of RyRs state changes is counted in each trial and each RyR is associated with its distance to LCC or the central RyR. The individual radial distance ($D(i,j)$) of each RyR ($ryr_{i,j}$) to the calcium release source (either the LCC or the central RyR in the two models) is simply the Euclidean distance. For better data processing, the distance is rounded up to the unit of 1 nm as follows:

$$d = \lceil D(i,j) \rceil = \left\lceil \sqrt{(x_{ryr\,i,j} - X)^2 + (y_{ryr\,i,j} - Y)^2 + (z_{ryr\,i,j} - Z)^2} \right\rceil \quad (1)$$

The activity occurrence number ($n(d)$) at a certain distance d (in nm) is the sum of all occurrence numbers of RyRs with the same distance d during the entire simulation course. Let i and j be the indices of the corresponding RyR:

$$n(d) = \sum_{i,j} n_{i,j}(d) \quad (2)$$

To reduce the random effects due to Monte Carlo simulations, the average of N trails is calculated by:

$$X^{avg}(d) = \frac{1}{N}\sum_{k=1}^{k=N} n^{(k)}(d), \qquad (3)$$

where N = 100 in our experiments. After the data processing using the above mathematical equations, the dependence of RyRs opening activities on the radial distance is rendered in the following figures.

A. LCC-RyR interaction with varying distance and time

Figure 5 shows that RyRs closer to LCC are more activated than the further ones. This is theoretically and objectively straightforward to understand. The comparison between different time durations, defined as the time period starting from the beginning of the simulation (or 0ms) to the time stamp specified in the figure, shows that the decreasing curves have steeper slopes within the first 10 ms.

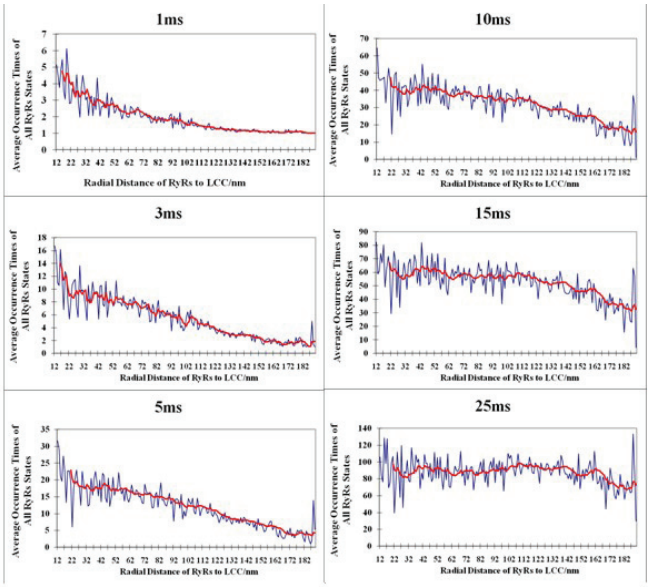

Figure 5 Patterns of RyRs activities with different radial distances to LCC depicted at different time durations. The *x*-axis is the distance (unit/1nm) and *y*-axis is average occurrence times of all RyRs states during the period from 0ms to the time steps specified in the figure.

After 10ms, however, the slopes get obvious fluctuations and the curves are significantly "flatter". At 25 ms, the curve becomes approximately horizontal, suggesting that LCC's influence on RyR activities gradually diminishes and becomes almost vanished after 25ms. To better observe the patterns of RyR activities spatially and temporarily, a three-dimensional graph is depicted in Figure 6. The difference between Figure 5 and 6 is that, in Figure 5 the time is a range, and the number of RyRs is cumulated activities of all RyRs, while every stripe in Figure 6 represents the pattern of RyR activities at a certain time point but not a time range from 0ms. Figure 6 suggests that at earlier time, the closer an RyR is to the LCC, the more kinetically active the RyR is. However, this tendency disappears or even reverses at later times for RyRs further to the opened LCC become more active due to RyR self-regeneration. This happens starting from 9~10ms as can be seen in Figure 6. This finding agrees with the fact that calcium sparks often occur

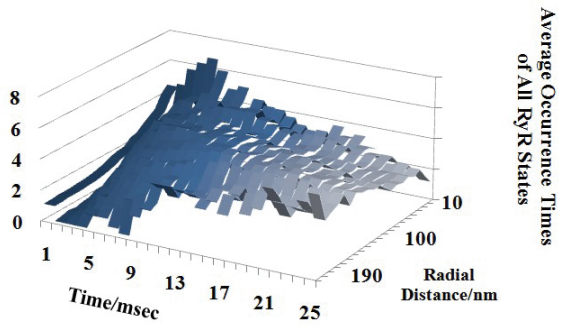

Figure 6 3-dimentioanl patterns of RyR activities. The time-axis is time stamps from 1ms to 25ms. The distance-axis shows the distance from RyRs to the opened LCC. The vertical axis reflects the average occurrence numbers of all RyRs activities with varying time steps and distances. Again, 100 experiments were conducted to reduce the random noise.

at ~10ms after the LCC opens. Many RyRs become hyperactive or open around the spark time, when the RyR self-stimulation has become more significant than the calcium release due directly to LCC's. Based on the above analysis, we observe that LCC triggering control is dominant before the spark but becomes much less important after the spark time.

B. RyRs self-control with varying distance and time

Figure 7 and Figure 8 show the activity patterns of RyRs with the distance to the initially opened RyR, which is considered as the source of this "cluster bomb" [6]. Similar to the experiments above, the time duration in Figure 7 is a range, while the time in Figure 8 is a specific time point.

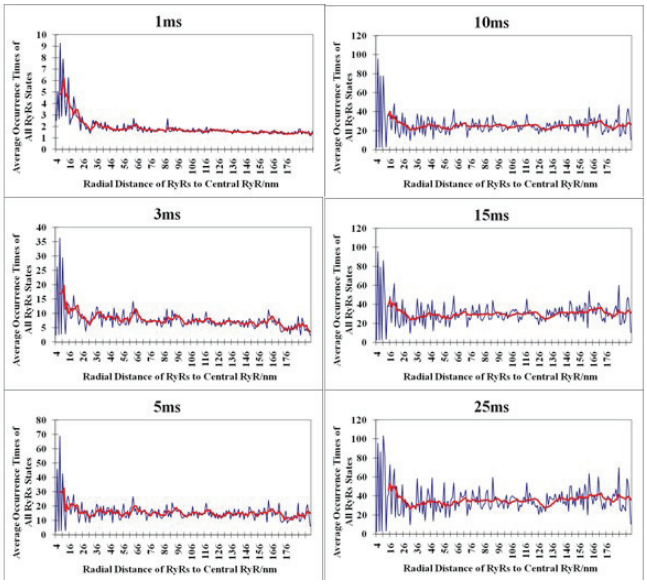

Figure 7 Patterns of RyRs activities with different radial distance to the initially opened RyR within different durations. *x* axis is the distance (unit/1nm) and *y* axis is the average occurrence times of all RyRs states.

The curves in Figure 7 rapidly decrease in the beginning, suggesting that an opened RyR only affects neighbors in a short distance. In addition, the initially opened RyR activates its neighboring RyRs in the cluster within a very short time. Subsequently, the opened channels activated by

the central RyR release calcium to trigger their adjacent RyRs. This RyR self-regeneration can be described as a "chain-reaction" process. The curves in Figure 7 stay roughly constant in the "tails", which suggests that the regeneration from one RyR to the neighbors propagates very fast. The three-dimensional graph of RyRs activities with both time and distance variations is shown in Figure 8, providing a more intuitively illustration. It implies that the influence of the initially opened RyR on other RyRs lessens with the radial distance before the spark formation around 5 ms (this can be seen clearly in Figure 8B). In this model, LCC triggering process is omitted; therefore the spark formation takes place much earlier than that where a LCC is included. Based on the observation, we conclude that the influence of the initially opened RyR's decreases with distance and rapidly vanishes after the spark formation. As time increases, RyRs further away become more active due to the fact that the RyRs near the center start to become inactive or closed (see Figure 2B). This mimics a wave from the center to the periphery of the simulation domain.

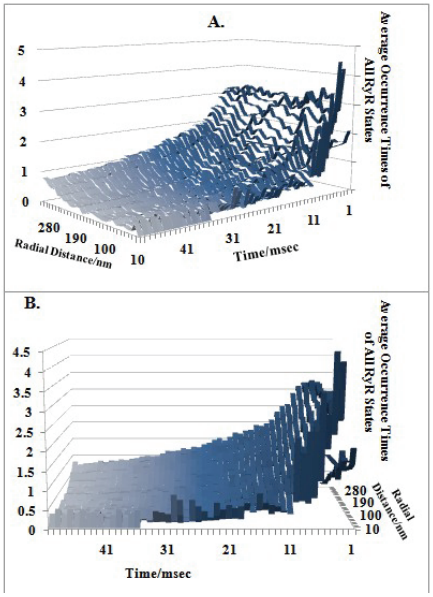

Figure 8 3-dimensional relations of RyRs activities with time and distance. The horizontal axis is time point. Total 50ms is observed. The vertical axis reflects the activities of RyRs, it is the average occurrence times of all RyRs states. The depth axis is the radial distance of RyRs to the central opened RyR.
(A) 3D vision from the perspective of 230 degree.
(B) 3D vision from the perspective of 90 degree.

C. *Time cost of the two controlling models above*

The time cost in Table1 includes the I/O time, especially writing the triggering outputs used to calculate the RyR activities. Time cost varies according to the number of excited (opened) RyRs. The longer the cost is, the more hyperactive RyRs are. Of course the size of the simulation domain as well as the number of membrane channels used is another factor that affects the computational cost.

Duration	Figure5	Figure7
1ms	44s	2m33s
3ms	3m34s	1h27m57s
5ms	16m45s	6h28m49s
10ms	32m15s	18h30m32s
15ms	2h14m16s	28h05m58s
25ms	4h38m04s	42h26m13s

Table 1 The computer time spent to conduct 100 independent simulation trials for different time durations in the two triggering models above. All experiments are performed with MCell on a Linux desktop with 2.0G RAM and a dual Intel CPU core at 3.00GHz.

IV. CONCLUSION

The main result of this study is that the influence of both LCCs and RyRs on other RyRs appears approximately inversely proportional to the radial distance when their triggering effects are dominant. LCC triggering influence vanishes after the spark formation. As for RyRs, the initial stimulation effect diminishes very quickly as more adjacent RyRs start to take in part in the self-regeneration process.

The models described allow us to study the effect of an individual LCC/RyR to calcium propagation. Nevertheless, in the real world, calcium signaling is the superposition of the effects of all the LCCs and RyRs. The principle of the superposition still remains to be explored. Meanwhile, the box models used are perhaps too simple from the biological point of view. Experiments using more realistic geometries, especially those extracted from 3D electron microscopy imaging data are under investigation.

ACKNOWLEDGEMENT: We thank Masahiko Hoshijima and Anushka Mihaylova for helpful discussions.

REFERENCES

[1] H. Cheng, W.J. Lederer, and M.B. Cannell, "Calcium Sparks: Elementary Events Underlying Excitation-Contraction Coupling in Heart Muscle," Science, vol. 262, pp. 740-744, 1993.
[2] Y. Fu, G. Zhang, X. Hao, C. Wu, Z. Chai, S. Wang, "Temperature Dependence and Thermodynamic Properties of Ca Sparks in Rat Cardiomyocytes," Biophys. J., vol. 89, pp. 2533-2541, 2005.
[3] J.D. Johnson, C. Snyder, M. Walsh, M. Flynn, "Effects of Myosin Light Chain Kinase and Peptides on Ca Exchange with the N- and C-terminal Ca Binding Sites of Calmodulin," J. of Biol. Chem., vol. 271, no.2, pp. 761-767, 1996.
[4] L.S. Song, S.Q. Wang, R.P Xiao, H. Spurgeon, Edward G. Lakatta, H. Cheng, "β−Adrenerigic Stimulation Synchronizes Intracellular Ca Release During Exicitation-Contraction Coupling in Cardiac Myoctyes," Circ. Res., vol. 88, pp. 794-801, 2001.
[5] X. Koh, B. Srinivasan, H.S. Ching, and A. Levchenko, "A 3D Monte Carlo Analysis of the Role of Dyadic Space Geometry in Spark Generation," Biophys. J., vol. 90, pp. 1999–2014, 2006.
[6] M.D. Stern, "Theory of excitation-contraction coupling in cardiac muscles," Biophys. J., vol. 63, pp. 497-517, 1992.
[7] P.H. Backx, Peiter P. De Tomebe, et.al., "A Model of Propagating Calcium-induced Calcium Release Mediated by Calcium Diffusion," The Journal of General Physiology, vol. 93, pp. 963–977, 1989.
[8] C. Franzini-Armstrong, F. Protasi, V. Ramesh, "Shape, size and distribution of Ca release Units and couplons in skeletal and cardiac muscles," Biophys. J., vol. 77, pp. 1528-1539, 1999.
[9] H. Takekura, and C. Franzini-Armstrong, "The Structure of Ca Release Units in Arthropod Body Muscle Indicates an Indirect Mechanism for Excitation-Contraction Coupling," Biophys. J., vol. 83, pp. 2742–2753, 2002.
[10] G.A. Langer and A. Peskoff, "Calcium Concentration and Movement in the Dyadic Cleft Space of the Cardiac Ventricular Cell," Biophys. J., vol. 70, pp. 1169–1182, 1996.
[11] E.D. Moore, T. Voigt, Y.M. Kobayashi, G. Isenberg, F.S. Fay, M.F. Gallitelli, and C. Franzini-Armstrong, "Organization of Ca Release Units in Excitable Smooth Muscles of the Guinea-Pig Urinary Bladder," Biophys. J., vol. 87, pp. 1836-1847, 2004.
[12] G.S.B. Willams, M.A. Huertas, E.A. Sobie, M.S. Jafri, and G.D. Smith, "Moment closure for Local Control Models of Calcium-Induced Calcium Release in Cardiac Myocytes," Biophys. J., vol. 95, pp. 1689-1703, 2008.
[13] H. Cheng, W.J. Lederer, "Calcium Sparks," Physiol. Rev., vol. 88, pp. 1491–1545, 2008.
[14] J. Hake and G.T. Lines, "Stochastic Binding of Ca Ions in the Dyadic Cleft; Continuous versus Random Walk Description of Diffusion," Biophys. J., vol. 94, pp. 4184–4201, 2008.